PROCEEDINGS OF SCIENCE

Black-Hole Mergers

Michael Kesden*
Center for Cosmology and Particle Physics, New York University
4 Washington Pl., New York, NY 10003, USA
E-mail: mhk10@nyu.edu

Observations of black-hole mergers will provide unique insights into both general relativity and cosmology. The gravitational waves produced in such mergers directly probe strong-field solutions to Einstein's equations, and the rate at which mergers occur constrains the hierarchical formation of supermassive black holes and their host galaxies. The three primary theoretical tools for studying merging black holes are post-Newtonian expansions, black-hole perturbation theory, and numerical relativity. I will briefly explain how these tools complement each other in developing a general solution to the problem of black-hole mergers, highlighting some of my own research in each of these three areas.

Frank N. Bash Symposium New Horizons In Astronomy,
October 9-11, 2011
Austin Texas

*Speaker.

PoS(Bash11)007

1. Black holes

In 1915, Albert Einstein presented his famous field equation of general relativity

$$G_{\mu\nu} = 8\pi G T_{\mu\nu} \tag{1.1}$$

which relates the curvature of spacetime (described by the Einstein tensor $G_{\mu\nu}$) to the energy content of the universe (given by the stress-energy tensor $T_{\mu\nu}$). Roy Kerr discovered the unique *stationary, axisymmetric, vacuum* solution to this equation

$$ds^2 = -\left(1-\frac{2Mr}{\Sigma}\right)dt^2 - \frac{4Mar\sin^2\theta}{\Sigma}dtd\phi + \frac{\Sigma}{\Delta}dr^2 + \Sigma d\theta^2 + \left(r^2+a^2+\frac{2Ma^2r\sin^2\theta}{\Sigma}\right)\sin^2\theta d\phi^2 \tag{1.2}$$

where $\Sigma \equiv r^2 + a^2\cos^2\theta$ and $\Delta \equiv r^2 - 2Mr + a^2$ [1]. Classical black holes described by this Kerr metric are the simplest objects in the universe, fully described by their mass M and spin angular momentum $J = aM$ in relativist's units where $G = c = 1$.

Several of the distinguishing features of black holes are their event horizons, ergospheres, and innermost stable circular orbits [2]. The *event horizon* is the boundary of the region of spacetime that is causally disconnected from future null infinity. Even light rays cannot escape from inside the event horizon, hence the term "black holes." Spinning black holes have an *ergosphere* exterior to their event horizons within which all stationary observers must orbit the black hole with positive angular velocity. Negative-energy orbits also exist within the ergosphere, allowing rotational energy to be extracted from the black hole [3]. Black holes, unlike Newtonian point masses, also have *innermost stable circular orbits* (ISCOs). Massive particles inspiraling into black holes through gravitational radiation or viscous dissipation will plunge into the event horizons after reaching the ISCO.

Astrophysical black holes are formed in two distinct channels. *Stellar-mass* black holes are formed in the gravitational collapse of stars whose cores are too massive to be supported by electron or neutron degeneracy pressure. Oppenheimer and Snyder [4] performed the first calculation of this collapse into a black hole. Stellar-mass black holes can be observed if they accrete from a stellar binary companion. The accreted material can be heated to temperatures high enough to emit copious X-rays; the nearby black-hole candidate Cygnus X-1 was discovered in a rocket-borne X-ray survey in 1964 [5]. The second kind of astrophysical black hole is the *supermassive* black holes (SBHs) that reside in the centers of most large galaxies. The Doppler broadened emission lines associated with active galactic nuclei (AGN) were discovered by Carl Seyfert in 1943 [6]. Twenty years later, theorists proposed that these AGN were powered by accretion onto compact objects of masses $10^5 - 10^8 M_\odot$ [7]. Such massive objects cannot support themselves against gravitational collapse into SBHs [8]. SBHs grow by accreting gas and merging with each other during the galaxy mergers through which large galaxies are assembled. We consider black-hole mergers in greater detail in the next section.

2. Black-hole mergers

As we learned in the last section, isolated black holes are simple objects that are fully described by their mass and spin. Widely separated binary black holes are similarly simple; they are

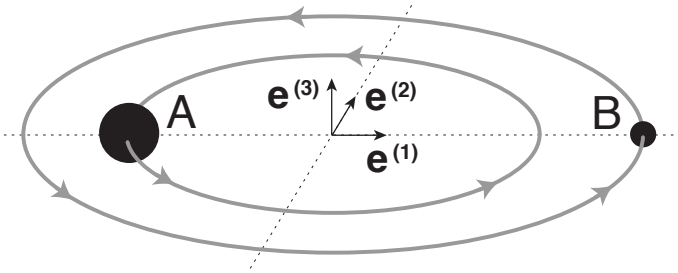

Figure 1: Binary black holes A and B on a quasi-circular orbit about their common center of mass. We define an orthonormal coordinate system such that at an initial time $\mathbf{e}^{(1)}$ points along the separation vector between the two holes, $\mathbf{e}^{(3)}$ points along the orbital angular momentum, and $\mathbf{e}^{(2)}$ completes the triad.

described by the mass and spin of the two black holes along with the orbital parameters of the binary. Any system with a time-varying mass-quadrupole moment, such as binary black holes, emits gravitational radiation that extracts energy and angular momentum from the system. This radiation circularizes the orbits of widely separated black holes [9], so for many purposes it is sufficient to restrict our attention to black holes on initially circular orbits. The reference frame we will use to describe the quasi-circular binary system is illustrated in Fig. 1. The Kerr metric given by Eq. (1.2) is scale-invariant when r and a are expressed in units of M, indicating that calculations involving the binary system can be rescaled to any desired value of the total mass. A general black-hole binary can therefore be described by 7 parameters: the binary mass ratio $q \equiv M_b/M_a \leq 1$ and the 3 components of the dimensionless spins $\mathbf{a}$ and $\mathbf{b}$ of black holes A and B.

Given this initial state, the black-hole merger proceeds in three stages. In the first stage, known as the *adiabatic inspiral*, the binary emits gravitational radiation that extracts energy and angular momentum from the orbit. The timescale $t_{\rm GW} \equiv E_{\rm orb}/\dot{E}_{\rm GW}$ for this orbital decay is much longer than the orbital time $t_{\rm orb} \simeq \Omega^{-1}$, so the binary evolves through a sequence of quasi-circular orbits of decreasing separation and increasing orbital frequency Ω. In the second stage, the *merger* itself, the individual event horizons of the binary black holes coalesce into a single perturbed horizon of the final black hole. In the final stage of the merger, the *ringdown*, the perturbed final black hole emits additional gravitational radiation until it settles down into an unperturbed Kerr black hole. This final black hole is fully characterized by its mass M_f, dimensionless spin $\mathbf{s}$, and recoil velocity $\mathbf{k}$ with respect to the center of mass of the initial binary.

We learned in the previous section that astrophysical black holes can be divided into stellar-mass black holes ($m \simeq 10M_\odot$) formed in the gravitational collapse of massive stars, and supermassive black holes ($10^6 M_\odot \lesssim m \lesssim 10^{10} M_\odot$) in galactic centers. This bimodality in the astrophysical black-hole population motivates us to distinguish between *comparable-mass* mergers for which $q \simeq 1$ and *extreme-mass-ratio inspirals* (EMRIs) for which $q \ll 1$. Comparable-mass mergers occur when both members of the binary are either stellar-mass black holes or supermassive black holes. These two different regimes of comparable-mass mergers can be analyzed with the same theoretical tools because of the scale-invariance of general relativity noted earlier. EMRIs occur when a supermassive black hole merges with a much smaller stellar-mass black hole. Different theoretical techniques must be used to study black-hole mergers in the limit $q \ll 1$ as will be discussed

in later sections.

Although general-relativity calculations are independent of the total binary mass, this scale greatly affects our ability to observe the mergers themselves. Current constraints on black-hole mergers and the rates at which they occur are inferred from observations of how the black-hole population evolves with time. We have never actually observed binary stellar-mass black holes, so our predictions about their merger rates are entirely theoretical. These predictions are plagued by uncertainties about how many main-sequence stars collapse into black holes, how these stars evolve in binaries, and how many new binaries can form in dense stellar environments. Predicted rates for stellar-mass black-hole mergers vary from 10^{-4} to 0.3 Mpc^{-3} Myr^{-1} [10]. The rate at which supermassive black holes merge is also uncertain. SBH masses are tightly correlated with the luminosity [11], mass [12], and velocity dispersion [13] of the spheroidal component of their host galaxies. If we assume that SBHs merge promptly following the mergers of their host galaxies, we can use observational and theoretical predictions of galaxy-merger rates to infer SBH merger rates. Unfortunately, this assumption may not be valid as neither dynamical friction nor gravitational radiation can cause SBHs separated by ~ 1 pc to merge within a Hubble time (the so-called "final parsec problem") [14]. Though there are several proposed solutions to the final parsec problem, the effectiveness of these solutions in a cosmological context has not been established. EMRI rates are also uncertain for several reasons. Mass segregation should cause stellar-mass black holes, heavier than average stars, to settle to the center of nuclear star clusters where they are susceptible to being scattered into "loss-cone" orbits on which they can merge with SBHs. Unfortunately, the time scale for this mass segregation depends sensitively on stellar densities at the center of nuclear star clusters. Recent observations suggest that the nuclear star cluster of our own Galaxy has a core with radius $r_0 \simeq 0.5$ pc [15], and that this core may inhibit the diffusion of $10M_\odot$ black holes onto loss-cone orbits [16]. Previously unappreciated relativistic dynamics may also reduce predicted EMRI rates by factors of $\sim 10-100$ below previous predictions [17].

The cleanest probe of black-hole mergers is the gravitational waves (GWs) produced during the inspiral, merger, and ringdown described above. GWs with frequencies $10\,\mathrm{Hz} \lesssim f \lesssim 10^4\mathrm{Hz}$ can be observed by the network of GW detectors operated by the Laser Interferometer Gravitational-wave Observatory (LIGO) [18] and the European Gravitational Observatory [19]. These frequencies correspond to the merger/ringdown stage of the merger of $\sim 200M_\odot$ black holes, or the inspiral stage of smaller comparable-mass ratio mergers. When Advanced LIGO achieves design sensitivity in ~ 2016, it should be able to detect GWs from the inspiral of $1.4M_\odot$ neutron stars out to distances of ~ 300 Mpc. The proposed Laser Interferometer Space Antenna (LISA) [20] would have observed GWs with frequencies $10^{-4}\mathrm{Hz} \lesssim f \lesssim 10^{-1}\mathrm{Hz}$ with enough sensitivity to detect the mergers of SBHs with $10^5 M_\odot \lesssim M \lesssim 10^7 M_\odot$ throughout the observable universe. LISA would also have seen thousands of EMRIs out to redshift $z \sim 1$. Although budgetary constraints have forced NASA and ESA to end the LISA collaboration, ESA is considering a European-only New Gravitational-wave Observatory (NGO) [21] as an L-class mission. NGO will have reduced S/N ratios compared to earlier LISA proposals, but should still be able to achieve many of LISA's core science goals. In the time domain, the expected GW strain from black-hole mergers is far below the design sensitivity of LIGO and NGO. GW sources can only be detected by convolving a predetermined template with the observed signal over many GW periods. Different theoretical methods are required to calculate these GW templates for the inspiral, merger, and ringdown stages in the

comparable-mass and EMRI limits. These methods will be the subject of the next section.

3. Strategic triad of general relativity

The three legs of the U. S. nuclear triad are long-range strategic bombers, land-based intercontinental ballistic missiles (ICBMs), and ballistic-missile submarines. These three weapons complement each other, and ensure that the U. S. maintains a credible second-strike capability in spite of any conceivable first-strike attack by enemy forces. There are also three primary techniques for performing calculations in general relativity: *numerical relativity*, *black-hole perturbation theory*, and *post-Newtonian expansions*. Like the nuclear triad, these techniques complement each other and ensure that suitable GW waveforms can be calculated for all three stages of black-hole mergers as discussed in the previous section. In the remainder of this section we will briefly discuss these techniques and illustrate their utility by provided examples from my own research of problems that they can be used to solve.

3.1 Numerical relativity

In the late 1990s, the NSF awarded a "Grand Challenge" grant to encourage research to simulate the merger of binary black holes by directly solving Einstein's equation Eq. (1.1). Despite much hard work on this problem during that decade, the merger of equal-mass binary black holes on initially quasi-circular orbits was not successfully simulated until Frans Pretorius accomplished the feat in 2005 [22]. Several other numerical-relativity (NR) groups successfully simulated black-hole mergers shortly thereafter [23, 24], and to date hundreds of black-hole simulations with varying mass ratios and initial spins have been published. NR simulations are the most general technique for calculating the GWs from binary black-hole mergers, and are the *only* technique that can accurately determine the waveform from the merger stage of comparable-mass mergers. Although all relativity problems could be solved with NR simulations in theory, in practice they can be prohibitively expensive computationally. The simplest NR simulations require 10^4 CPU-hours of computing resources, and their cost scales as q^{-2} for unequal-mass mergers. The smallest mass-ratio simulation currently published has $q = 0.01$ [25], and it seems unlikely that much progress beyond this limit will be achieved with current NR techniques. NR simulations are thus unsuited to EMRIs where $q \lesssim 10^{-5}$. Given the extraordinary computational expense of NR simulations, cleverness is required to extract the most information from a small sample of simulations.

My collaborators and I developed a new spin expansion that exploits symmetry to determine the general spin dependence of GW observables from a finite number of NR simulations [26, 27]. All final quantities f that describe the final black hole produced in a merger can only depend on the 7 parameters $\{q, a_i, b_i\}$ that characterize the initial binary (see Fig. 1). Since the magnitudes of the dimensionless spin of Kerr black holes cannot exceed unity ($|a_i|, |b_i| \leq 1$), these final quantities can be Taylor expanded in terms of the initial spin components:

$$f = f^{m_1 m_2 m_3 | n_1 n_2 n_3}(q) a_1^{m_1} a_2^{m_2} a_3^{m_3} b_1^{n_1} b_2^{n_2} b_3^{n_3} \, , \tag{3.1}$$

where summation over the repeated indices m_i, n_i is implied. This spin expansion is itself not very predictive, as the number of terms at each order in the initial spin components increases rapidly and

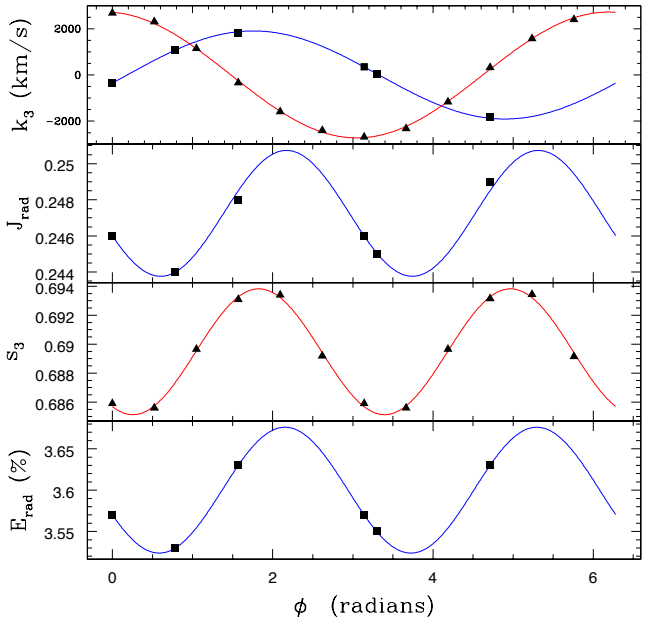

Figure 2: Kick velocity k_3, radiated angular momentum $J_{\rm rad}$, final spin s_3, and radiated energy $E_{\rm rad}$ as a function of the angle ϕ between the initial spin $\mathbf{a}$ and the coordinate vector $\mathbf{e}^{(1)}$ for equal-mass black-hole binaries with equal and opposite spins in the orbital plane. The square (triangle) data points are from [28] ([29]), while the functional form of the fitted curves are the lowest-order predictions of the spin expansion.

there is no guarantee that the series will quickly converge. However, considerable progress can be achieved by recognizing that the parameters $\{q,\mathbf{a},\mathbf{b}\}$ that define the initial binary, the orthonormal triad $\mathbf{e}^{(i)}$, and the final quantities $\{m,\mathbf{s},\mathbf{k}\}$ all transform in well defined way under the operations of parity P (reflection through the origin) and exchange X (exchanging the black-hole labels A and B). Because evolution according to Einstein's equation respects these symmetries, final quantities that transform in a given way under P and X can only depend on initial quantities that transform in the *same* manner. This dramatically reduces the number of terms that appear in the spin expansion of a particular quantity. We find that in practice the very lowest-order terms often provide an extremely accurate description of the desired spin dependence. This can be seen in Fig. 2, where various final quantities determined by NR simulations as a function of initial spin direction are compared to the predictions of the spin expansion. We see that final quantities $(J_{\rm rad},s_3,E_{\rm rad})$ that are scalars (even under parity P) are determined to lowest order to scale quadratically in the initial spins and to have frequencies of 2 as predicted by our formalism. In contrast, the pseudoscalars (quantities odd under P) such as the kick velocity k_3 are permitted to have a linear spin dependence with unit frequency.

The spin expansion not only explained previously discovered spin dependence, but also uncovered new spin dependence that had been previously unappreciated. In Fig. 3 we show the residuals Δk_3 after the best lowest-order fits using the spin expansion are subtracted from the top panel of Fig. 2. As predicted by symmetry, quadratic terms in the initial spins with frequency 2 are absent, with the dominant term being cubic in the spin amplitude and having frequency 3. This example

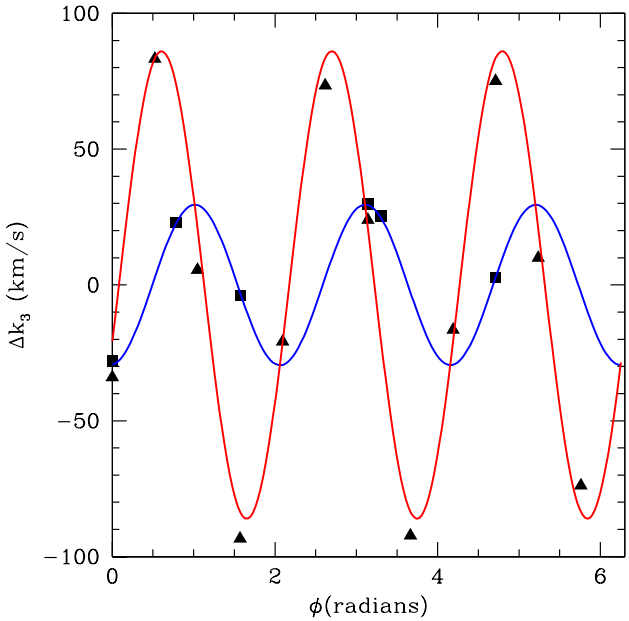

Figure 3: The residuals Δk_3 after the lowest-order spin-expansion fits are subtracted from the simulated kick velocities shown in Fig. 2. As shown by the fitted curves, these residuals are cubic in the spin magnitudes and have frequencies of 3 as predicted by our spin expansion.

illustrates both the power of NR simulations, and how this power can be best harnessed by using a small number of NR simulations to calibrate judicious fitting formulae such as our spin expansion. Our approach has been used extensively by other groups seeking to interpret their latest NR results.

3.2 Black-hole perturbation theory

Despite the extraordinary recent progress in NR, its computational expense and restriction to modest mass ratios ($q \gtrsim 0.1$) and SBH spins ($a/m \lesssim 0.9$) implies that it is not always the best technique for solving certain GR problems. EMRIs can instead be studied with *black-hole perturbation theory*, in which the smaller black hole and its accompanying gravitational radiation are treated as perturbations to the background metric of the larger black hole. Black-hole perturbation theory for the nonspinning Schwarzschild metric was introduced by Regge and Wheeler [30] and Zerilli [31] for odd- and even-parity perturbations respectively, and generalized to the spinning Kerr metric by Teukolsky [32]. Teukolsky showed that vacuum perturbations to the Kerr spacetime are fully described by the complex Weyl scalar

$$\psi_4 \equiv -C_{\alpha\beta\gamma\delta} n^\alpha \bar{m}^\beta n^\gamma \bar{m}^\delta \ , \tag{3.2}$$

where $C_{\alpha\beta\gamma\delta}$ is the Weyl curvature tensor and n^μ and $\bar{m}^\mu$ are elements of a Newman-Penrose tetrad of null 4-vectors [33]. This Weyl scalar can be decomposed into multipole moments

$$\psi_4(t,r,\theta,\phi) = \frac{1}{(r-ia\cos\theta)^4} \int_{-\infty}^{\infty} d\omega \sum_{lm} R_{lm\omega}(r)\, {}_{-2}S^{a\omega}_{lm}(\theta) e^{im\phi} e^{-i\omega t} \ , \tag{3.3}$$

where ${}_{-2}S^{a\omega}_{lm}(\theta)$ are generalizations of the Legendre functions that appear in ordinary spherical harmonics and $R_{lm\omega}(r)$ are radial functions that are solutions to the Teukolsky equation

$$\Delta^2 \frac{d}{dr}\left(\frac{1}{\Delta}\frac{dR_{lm\omega}}{dr}\right) - V(r)R_{lm\omega}(r) = \mathscr{T}_{lm\omega}(r) \; . \tag{3.4}$$

The potential $V(r)$ is a known analytic function for each harmonic, implying that the left-hand side of Eq. (3.4) depends solely on the spacetime curvature. The source term $\mathscr{T}_{lm\omega}(r)$ is an integral of the stress-energy tensor of the perturbation over the spacetime. The Teukolsky equation (3.4) is thus a linearization of Einstein's equation (1.1) in which 10 coupled, nonlinear, partial differential equations have been reduced to an infinite series of ordinary differential equations, one for each harmonic of the Weyl scalar. In practice, it is often the case that only a small number of harmonics are required to achieve the desired accuracy in a given GR calculation. Unlike NR, black-hole perturbation theory improves in accuracy as q decreases, and can be used for arbitrarily high spins. It is the technique of choice for studying EMRIs during the late inspiral, merger, and ringdown stages.

One application of black-hole perturbation theory in my own research was to calculate the maximum spin black holes can attain in binary mergers [34]. Bardeen [35] famously showed that a nonspinning black hole, accreting material from its prograde equatorial ISCO, could spin up to the Kerr limit ($a/M = 1$) after increasing its mass by a factor of $\sqrt{6}$ but could not surpass this limit. However, this analysis failed to account for what happens to the energy and angular momentum that must be lost to allow material to reach the ISCO. Thorne [36] showed that if this material is viscously transported to the ISCO through a standard thin accretion disk [37], the black hole would preferentially capture radiated photons with negative angular momentum with respect to the direction of the black hole's spin. This captured radiation would decrease the black hole's spin so that a limiting spin of only $a/m \simeq 0.998$ could be attained. Although this seems close to the Kerr limit, the gravitational binding energy at the ISCO increases sharply with black-hole spin so that the radiative efficiency of a black hole with $a/m \simeq 0.998$ is only $\eta \simeq 0.3$ compared to $\eta \simeq 0.42$ in the Kerr limit. I wondered if a similar limit might exist for black holes grown through binary mergers instead of gas accretion. During binary mergers it is gravitational radiation rather than viscous dissipation that extracts energy and angular momentum from the inspiraling material. Unlike the radiated photons studied by Thorne, whose short wavelengths imply that they travel on null geodesics of the Kerr metric, the GWs emitted during the inspiral have wavelengths comparable to the orbital radii of the inspiraling black hole and thus larger than the event horizon. This allows the GWs to be *superradiantly* scattered by the gravitational potential of the Kerr black hole, gaining amplitude before escaping to infinity. Superradiant scattering is an example of a Penrose process [3] in which rotational energy and angular momentum are extracted from a spinning black hole. Using GREMLIN (Gravitational Radiation in the Extreme Mass ratio LIMit), a black-hole perturbation theory code developed by Scott Hughes [38], I calculated the GW fluxes of energy and angular momentum both out to infinity and down to the event horizon during an EMRI. We show the effect of this superradiant scattering on the black hole's spin in Fig. 4. Highly spinning black holes rapidly spin up to the Kerr limit without accounting for superradiant scattering as shown by the dashed blue curves. Once the effects of scattering are included, only a limiting spin

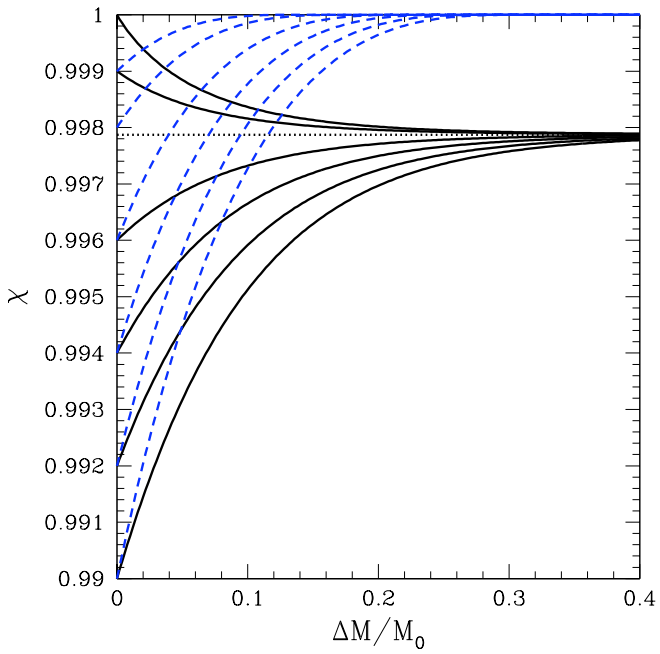

Figure 4: Dimensionless spin $\chi \equiv a/m$ of a black hole of initial mass M_0 after accreting a mass ΔM of test particles on quasi-circular prograde equatorial orbits. The different curves correspond to different values of the initial spin. The dashed blue curves show the predictions of Bardeen [35] that only include the spin dependence of the orbital energy and angular momentum at the ISCO, while the solid black curves also include the effects of the superradiant scattering of GWs as discussed in Kesden *et al.* [34].

$\chi \equiv a/m \simeq 0.998$ can be attained. The numerical value of this limit is quite close to the Thorne limit [36], although the processes setting these limits are quite different.

Predictions of the final spin resulting from EMRIs calculated using black-hole perturbation theory complement the predictions obtained from NR for comparable-mass mergers. In Fig. 5 we show the change in final spin per unit test-particle mass $\partial\chi_f/\partial q$ as a function of the initial spin χ_i. The solid black curve shows the prediction of Kesden *et al.* [34] that a black hole can only be spun up to $a/m \simeq 0.998$ by binary mergers, while the green and magenta curves, derived from extrapolations of comparable-mass NR simulations, erroneously suggest that black holes can be spun above the Kerr limit. This plot indicates that danger of relying exclusively on NR; all three techniques in the strategic triad of general relativity have their role to play in understanding black-hole mergers.

3.3 Post-Newtonian expansions

The final technique in the strategic triad of general relativity is the post-Newtonian (PN) expansion. PN expansions describing a system rapidly converge when the PN parameter $\varepsilon \approx (v/c)^2 \approx Gm/r \approx (M\omega)^{2/3} \ll 1$, where ω is the angular velocity. PN expansions are thus ideally suited to describing widely separated binary black holes, regardless of their mass ratio or the magnitude of their spins. PN expansions are the most computationally affordable of the three techniques con-

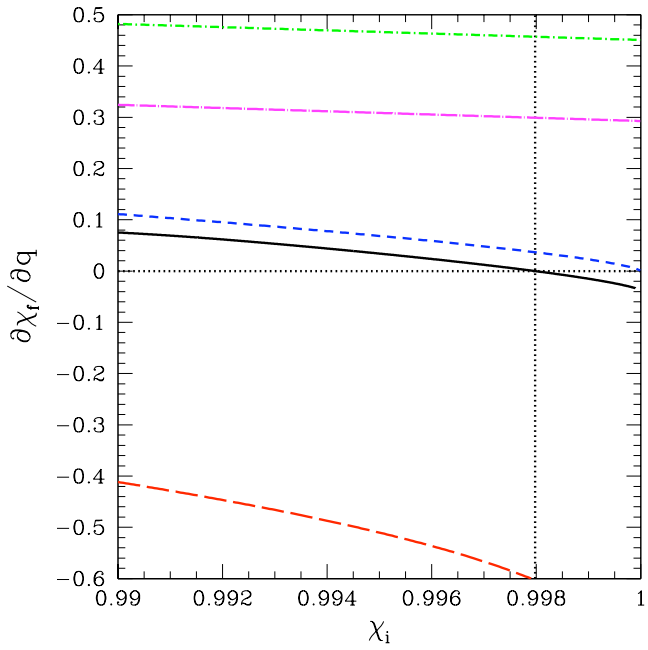

Figure 5: The change in final spin per unit test-particle mass $\partial\chi_f/\partial q$ as a function of the initial spin χ_i. The solid black curve shows the predictions of Kesden *et al.* [34], with spindown ($\partial\chi_f/\partial q \leq 0$, horizontal dotted line) possible for spins $\chi_i \geq \chi_{\rm lim}$ (vertical dotted line). The short-dashed blue curve shows how this result changes when superradiant scattering is neglected as in the models of Bardeen [35]. The long-dashed red curve gives the Buonanno *et al.* [39] prediction, while the dot-short-dashed green and dot-long-dashed magenta curves are the predictions of the NR-calibrated fitting formulae of Barausse and Rezzolla [40] and Tichy and Marronetti [41].

sidered in this section, so they should be the preferred technique during the inspiral stage of the merger. Discussion of the derivation of various PN expansions is beyond the scope of this work; I will instead focus on one particular application from my own research, the alignment of black-hole spins prior to merger.

As seen in the subsection on NR, the final spins and recoil velocities of black holes produced in mergers depend sensitively on the orientation of the initial binary black-hole spins just prior to merger. Tidal torques exerted by a circumbinary disk can extract orbital angular momentum from a black-hole binary, bringing the black holes close enough together to merge [14]. These same tidal torques can cause the black-hole spins to align with the angular momentum of the circumbinary disk [42], though it is unclear in practice how efficient this mechanism will be. At binary separations of $r_{\rm GW} \lesssim 3000M$, the torque exerted on the binary by gravitational radiation exceeds the tidal torque from the circumbinary disk. The evolution of the binary at $r \leq r_{\rm GW}$ becomes a pure general-relativity problem, one that is ideally suited to a PN analysis. Schnittman [43] discovered the existence of PN spin-orbit resonances into which black-hole binaries could become trapped, aligning their spins into special configurations. My collaborators and I [44, 45] showed that these resonances, acting on the astrophysically determined partially aligned spin configurations at $r \simeq r_{\rm GW}$, could align the spins in such a way as to profoundly influence the predicted distribu-

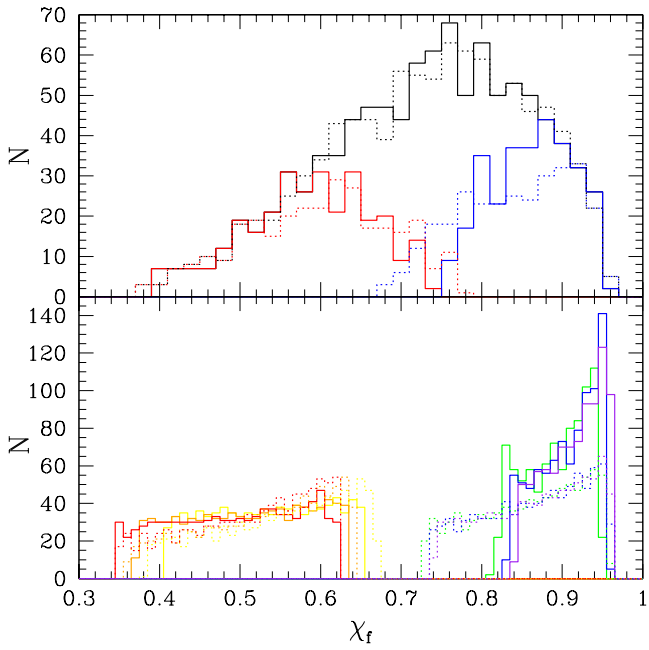

Figure 6: Histograms of the final spins predicted by the NR formula of [40] for black hole binaries with a mass ratio of $q = 9/11$ and different initial orientations of maximal spins. The dashed curves show the predictions assuming the spins remain in their initial orientations throughout the inspiral, while the solid curves include the effects of PN evolution for $r \leq 1000M$. In the top panel, the black distribution assumes isotropic initial spins for both black holes, while the blue (red) subset corresponds to the 30% of the distribution with the smallest (largest) initial angle between the spin of the more massive black hole and the orbital angular momentum. In the bottom panel, the smaller black hole has an initially isotropic spin distribution while the spin of the larger black hole is at an initial angle of 10° (purple), 20° (blue), 30° (green), 150° (yellow), 160° (orange), 170° (red) with respect to the orbital angular momentum.

tions of final spins and recoil velocities. In Fig. 6 we show how PN spin-orbit resonances affect the predicted distribution of final spins. The dominant effect is for the two initial spins to become aligned *with each other* when the larger spin is initially more closely aligned with the orbital angular momentum. This can be most clearly seen in the bottom panel, when comparing the solid and dashed distributions for the green, blue, and purple curves. Alignment of the binary spins with each other causes them to add coherently at merger, leading to a black hole with a larger final spin.

PN spin-orbit resonances have an even greater effect on the distribution of recoil velocities imparted to the final black hole. We show this effect in the histograms of Fig. 7. NR simulations show that recoil velocities are maximized when the black-hole spins are anti-aligned with each other just prior to merger [46]. Since the dominant effect of PN spin-orbit resonances is to align (anti-align) the binary spins with each other when the larger (smaller) black hole is more closely aligned with the orbital angular momentum, the recoil velocities will be suppressed (enhanced) in these cases. This is what is seen in Fig. 7; the recoil velocities are suppressed (enhanced) in the middle (bottom) panels. Most large galaxies are observed to host SBHs in their centers, which is seemingly at odds with the predictions of NR which suggest that recoils substantially exceeding

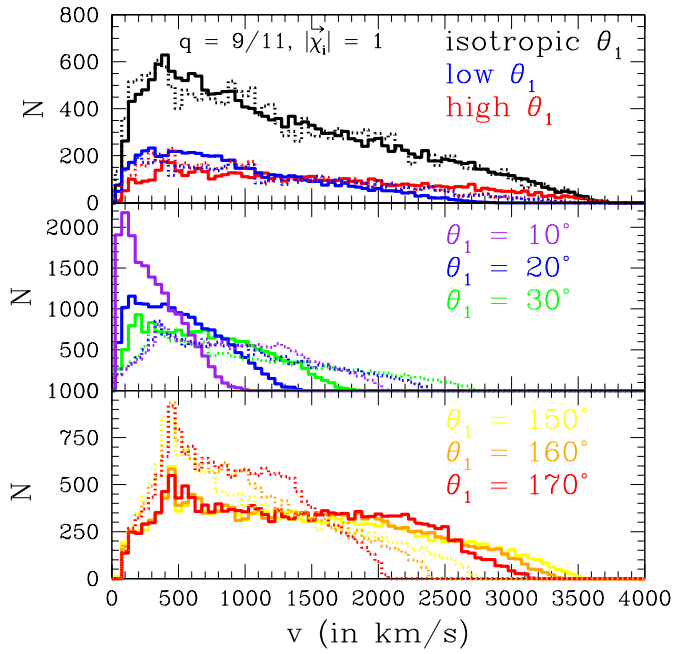

Figure 7: Histograms of the final recoils predicted by the NR formula of [46] for a mass ratio of $q = 9/11$ and different initial spin configurations. The curves in the top panel correspond to the same initial spin distributions as in the top panel of Fig. 6, while the curves in the middle and lower panels correspond to the curves in the lower panel of Fig. 6.

galactic escape velocities are generic. The effects of PN spin-orbit resonances that we discovered may help reconcile theory with observation.

4. Summary

Black-hole mergers occur throughout our universe, and provide a unique opportunity to test the predictions of Einstein's theory of general relativity. Black holes are observed to have a bimodal distribution of masses: stellar-mass black holes formed from the gravitational collapse of high-mass stars, and supermassive black holes grown through gas accretion and mergers in galactic centers. The mergers of these black holes can be distinguished into comparable-mass mergers and extreme mass-ratio inspirals (EMRIs). The mergers themselves can be separated into three stages: adiabatic inspiral, merger, and ringdown. There are three primary tools (the strategic triad of general relativity) that can be used to understand different stages of the merger. Numerical relativity is very computationally expensive but is the only tool that can be used to model the "merger" stage for comparable-mass mergers. Black-hole perturbation theory can be used for all stages of the EMRIs, where the smaller black hole and its accompanying gravitational radiation can be considered to be perturbations about the background Kerr spacetime of the larger black hole. Post-Newtonian expansions are the most computationally affordable, and can be used when velocities are not highly relativistic and the curvature is not extreme. They are ideally suited to

describing the early inspiral stage of mergers. To understand black-hole mergers in full generality, we must master all these tools and use them to complement each other.

References

[1] R. P. Kerr, *Gravitational field of a spinning mass as an example of algebraically special metrics*, Phys. Rev. Lett. **11**, 237 (1963).

[2] C. W. Misner, K. S. Thorne and J. A. Wheeler, *Gravitation*, W. H. Freeman and Company, New York, (1973).

[3] R. Penrose, *Gravitational collapse: The role of general relativity*, Riv. Nuovo Cim. **1**, 252 (1969) [Gen. Rel. Grav. **34**, 1141 (2002)].

[4] J. R. Oppenheimer and H. Snyder, *On Continued gravitational contraction*, Phys. Rev. **56**, 455 (1939).

[5] S. Bowyer, E. T. Byram, T. A. Chubb and H. Friedman, *Cosmic X-ray sources*, Science **147**, 394 (1965).

[6] C. Seyfert, *Nuclear emission in spiral nebulae*, Astrophys. J. **97**, 28 (1943).

[7] F. Hoyle, W. A. Fowler, *On the nature off strong radio sources*, Mon. Not. Roy. Astron. Soc. **125**, 169 (1963).

[8] D. Lynden-Bell, *Galactic nuclei as collapsed old quasars*, Nature **223**, 690 (1969).

[9] P. C. Peters and J. Mathews, *Gravitational radiation from point masses in a Keplerian orbit*, Phys. Rev. **131**, 435 (1963).

[10] J. Abadie *et al.* [LIGO Scientific and Virgo Collaborations], *Predictions for the Rates of Compact Binary Coalescences Observable by Ground-based Gravitational-wave Detectors*, Class. Quant. Grav. **27**, 173001 (2010).

[11] J. Kormendy, D. Richstone, *Inward bound: The Search for supermassive black holes in galactic nuclei*, Ann. Rev. Astron. Astrophys. **33**, 581 (1995).

[12] J. Magorrian, S. Tremaine, D. Richstone, R. Bender, G. Bower, A. Dressler, S. M. Faber, K. Gebhardt *et al.*, *The Demography of massive dark objects in galaxy centers*, Astron. J. **115**, 2285 (1998).

[13] K. Gebhardt, R. Bender, G. Bower, A. Dressler, S. M. Faber, A. V. Filippenko, R. Green, C. Grillmair *et al.*, *A Relationship between nuclear black hole mass and galaxy velocity dispersion*, Astrophys. J. **539**, L13 (2000).

[14] M. C. Begelman, R. D. Blandford and M. J. Rees, *Massive black hole binaries in active galactic nuclei*, Nature **287**, 307 (1980).

[15] R. M. Buchholz, R. Schodel, A. Eckart, *Composition of the galactic center star cluster: Population analysis from adaptive optics narrow band spectral energy distributions*, Astron. Astrophys. **499**, 483 (2009).

[16] D. Merritt, *The Distribution of Stars and Stellar Remnants at the Galactic Center*, Astrophys. J. **718**, 739 (2010).

[17] D. Merritt, T. Alexander, S. Mikkola and C. M. Will, *Stellar Dynamics of Extreme-Mass-Ratio Inspirals*, Phys. Rev. D **84**, 044024 (2011).

[18] LIGO - Laser Interferometer Gravitational Wave Observatory, http://www.ligo.caltech.edu/.

[19] Virgo, https://wwwcascina.virgo.infn.it/.

[20] LISA - Laser Interferometer Space Antenna, http://lisa.nasa.gov/.

[21] ESA Science & Technology: Next steps for LISA, http://sci.esa.int/science-e/www/object/index.cfm?fobjectid=48728

[22] F. Pretorius, *Evolution of binary black hole spacetimes*, Phys. Rev. Lett. **95**, 121101 (2005).

[23] M. Campanelli, C. O. Lousto, P. Marronetti and Y. Zlochower, *Accurate evolutions of orbiting black-hole binaries without excision*, Phys. Rev. Lett. **96**, 111101 (2006).

[24] J. G. Baker, J. Centrella, D. -I. Choi, M. Koppitz and J. van Meter, *Gravitational wave extraction from an inspiraling configuration of merging black holes*, Phys. Rev. Lett. **96**, 111102 (2006).

[25] C. O. Lousto and Y. Zlochower, *Orbital Evolution of Extreme-Mass-Ratio Black-Hole Binaries with Numerical Relativity*, Phys. Rev. Lett. **106**, 041101 (2011).

[26] L. Boyle, M. Kesden and S. Nissanke, *Binary black hole merger: Symmetry and the spin expansion*, Phys. Rev. Lett. **100**, 151101 (2008).

[27] L. Boyle and M. Kesden, *The spin expansion for binary black hole merger: new predictions and future directions*, Phys. Rev. D **78**, 024017 (2008).

[28] M. Campanelli, C. O. Lousto, Y. Zlochower and D. Merritt, *Maximum gravitational recoil*, Phys. Rev. Lett. **98**, 231102 (2007).

[29] B. Bruegmann, J. A. Gonzalez, M. Hannam, S. Husa and U. Sperhake, *Exploring black hole superkicks*, Phys. Rev. D **77**, 124047 (2008).

[30] T. Regge and J. A. Wheeler, *Stability of a Schwarzschild singularity*, Phys. Rev. **108**, 1063 (1957).

[31] F. J. Zerilli, *Gravitational field of a particle falling in a schwarzschild geometry analyzed in tensor harmonics*, Phys. Rev. D **2**, 2141 (1970).

[32] S. A. Teukolsky, *Perturbations of a rotating black hole. 1. Fundamental equations for gravitational electromagnetic and neutrino field perturbations*, Astrophys. J. **185**, 635 (1973).

[33] E. Newman and R. Penrose, *An Approach to gravitational radiation by a method of spin coefficients*, J. Math. Phys. **3**, 566 (1962).

[34] M. Kesden, G. Lockhart and E. S. Phinney, *Maximum black-hole spin from quasi-circular binary mergers*, Phys. Rev. D **82**, 124045 (2010).

[35] J. M. Bardeen, *Kerr metric black holes*, Nature **226**, 64 (1970).

[36] K. S. Thorne, *Disk Accretion Onto A Black Hole. 2. Evolution Of The Hole*, Astrophys. J. **191**, 507 (1974).

[37] N. I. Shakura and R. A. Sunyaev, *Black holes in binary systems. Observational appearance*, Astron. Astrophys. **24**, 337 (1973).

[38] S. A. Hughes, *The evolution of circular, non-equatorial orbits of Kerr black holes due to gravitational-wave emission*, Phys. Rev. D **61**, 084004 (2000) [Erratum-ibid. D **63**, 049902 (2001 ERRAT,D65,069902.2002 ERRAT,D67,089901.2003)].

[39] A. Buonanno, L. E. Kidder and L. Lehner, *Estimating the final spin of a binary black hole coalescence*, Phys. Rev. D **77**, 026004 (2008).

[40] E. Barausse and L. Rezzolla, *Predicting the direction of the final spin from the coalescence of two black holes*, Astrophys. J. **704**, L40 (2009).

[41] W. Tichy and P. Marronetti, *The final mass and spin of black hole mergers*, Phys. Rev. D **78**, 081501 (2008).

[42] T. Bogdanovic, C. S. Reynolds and M. C. Miller, *Alignment of the spins of supermassive black holes prior to merger*, Astrophys. J. **661**, L147 (2007).

[43] J. D. Schnittman, *Spin-orbit resonance and the evolution of compact binary systems*, Phys. Rev. D **70**, 124020 (2004).

[44] M. Kesden, U. Sperhake and E. Berti, *Final spins from the merger of precessing binary black holes*, Phys. Rev. D **81**, 084054 (2010).

[45] M. Kesden, U. Sperhake and E. Berti, *Relativistic Suppression of Black Hole Recoils*, Astrophys. J. **715**, 1006 (2010).

[46] M. Campanelli, C. O. Lousto, Y. Zlochower and D. Merritt, *Large merger recoils and spin flips from generic black-hole binaries*, Astrophys. J. **659**, L5 (2007).